School of Natural Sciences and Mathematics

Observation of the Helicity-Selection-Rule Suppressed Decay of the χ$_{c2}$ Charmonium State

UT Dallas Author(s):

Xinchou Lou

Observation of the helicity-selection-rule suppressed decay of the χ_{c2} charmonium state

M. Ablikim,[1] M. N. Achasov,[9,e] S. Ahmed,[14] X. C. Ai,[1] O. Albayrak,[5] M. Albrecht,[4] D. J. Ambrose,[44] A. Amoroso,[49a,49c] F. F. An,[1] Q. An,[46,a] J. Z. Bai,[1] O. Bakina,[23] R. Baldini Ferroli,[20a] Y. Ban,[31] D. W. Bennett,[19] J. V. Bennett,[5] N. Berger,[22] M. Bertani,[20a] D. Bettoni,[21a] J. M. Bian,[43] F. Bianchi,[49a,49c] E. Boger,[23,c] I. Boyko,[23] R. A. Briere,[5] H. Cai,[51] X. Cai,[1,a] O. Cakir,[40a] A. Calcaterra,[20a] G. F. Cao,[1] S. A. Cetin,[40b] J. Chai,[49c] J. F. Chang,[1,a] G. Chelkov,[23,c,d] G. Chen,[1] H. S. Chen,[1] J. C. Chen,[1] M. L. Chen,[1,a] S. Chen,[41] S. J. Chen,[29] X. Chen,[1,a] X. R. Chen,[26] Y. B. Chen,[1,a] X. K. Chu,[31] G. Cibinetto,[21a] H. L. Dai,[1,a] J. P. Dai,[34,j] A. Dbeyssi,[14] D. Dedovich,[23] Z. Y. Deng,[1] A. Denig,[22] I. Denysenko,[23] M. Destefanis,[49a,49c] F. De Mori,[49a,49c] Y. Ding,[27] C. Dong,[30] J. Dong,[1,a] L. Y. Dong,[1] M. Y. Dong,[1,a] Z. L. Dou,[29] S. X. Du,[53] P. F. Duan,[1] J. Z. Fan,[39] J. Fang,[1,a] S. S. Fang,[1] X. Fang,[46,a] Y. Fang,[1] R. Farinelli,[21a,21b] L. Fava,[49b,49c] F. Feldbauer,[22] G. Felici,[20a] C. Q. Feng,[46,a] E. Fioravanti,[21a] M. Fritsch,[14,22] C. D. Fu,[1] Q. Gao,[1] X. L. Gao,[46,a] Y. Gao,[39] Z. Gao,[46,a] I. Garzia,[21a] K. Goetzen,[10] L. Gong,[30] W. X. Gong,[1,a] W. Gradl,[22] M. Greco,[49a,49c] M. H. Gu,[1,a] Y. T. Gu,[12] Y. H. Guan,[1] A. Q. Guo,[1] L. B. Guo,[28] R. P. Guo,[1] Y. Guo,[1] Y. P. Guo,[22] Z. Haddadi,[25] A. Hafner,[22] S. Han,[51] X. Q. Hao,[15] F. A. Harris,[42] K. L. He,[1] F. H. Heinsius,[4] T. Held,[4] Y. K. Heng,[1,a] T. Holtmann,[4] Z. L. Hou,[1] C. Hu,[28] H. M. Hu,[1] T. Hu,[1,a] Y. Hu,[1] G. S. Huang,[46,a] J. S. Huang,[15] X. T. Huang,[33] X. Z. Huang,[29] Z. L. Huang,[27] T. Hussain,[48] W. Ikegami Andersson,[50] Q. Ji,[1] Q. P. Ji,[15] X. B. Ji,[1] X. L. Ji,[1,a] L. W. Jiang,[51] X. S. Jiang,[1,a] X. Y. Jiang,[30] J. B. Jiao,[33] Z. Jiao,[17] D. P. Jin,[1,a] S. Jin,[1] T. Johansson,[50] A. Julin,[43] N. Kalantar-Nayestanaki,[25] X. L. Kang,[1] X. S. Kang,[30] M. Kavatsyuk,[25] B. C. Ke,[5] P. Kiese,[22] R. Kliemt,[10] B. Kloss,[22] O. B. Kolcu,[40b,h] B. Kopf,[4] M. Kornicer,[42] A. Kupsc,[50] W. Kühn,[24] J. S. Lange,[24] M. Lara,[19] P. Larin,[14] H. Leithoff,[22] C. Leng,[49c] C. Li,[50] Cheng Li,[46,a] D. M. Li,[53] F. Li,[1,a] F. Y. Li,[31] G. Li,[1] H. B. Li,[1] H. J. Li,[1] J. C. Li,[1] Jin Li,[32] K. Li,[13] K. Li,[33] Lei Li,[3] P. R. Li,[7,41] Q. Y. Li,[33] T. Li,[33] W. D. Li,[1] W. G. Li,[1] X. L. Li,[33] X. N. Li,[1,a] X. Q. Li,[30] Y. B. Li,[2] Z. B. Li,[38] H. Liang,[46,a] Y. F. Liang,[36] Y. T. Liang,[24] G. R. Liao,[11] D. X. Lin,[14] B. Liu,[34,j] B. J. Liu,[1] C. X. Liu,[1] D. Liu,[46,a] F. H. Liu,[35] Fang Liu,[1] Feng Liu,[6] H. B. Liu,[12] H. H. Liu,[1] H. H. Liu,[16] H. M. Liu,[1] J. Liu,[1] J. B. Liu,[46,a] J. P. Liu,[51] J. Y. Liu,[1] K. Liu,[39] K. Y. Liu,[27] L. D. Liu,[31] P. L. Liu,[1,a] Q. Liu,[41] S. B. Liu,[46,a] X. Liu,[26] Y. B. Liu,[30] Y. Y. Liu,[30] Z. A. Liu,[1,a] Zhiqing Liu,[22] H. Loehner,[25] Y. F. Long,[31] X. C. Lou,[1,a,g] H. J. Lu,[17] J. G. Lu,[1,a] Y. Lu,[1] Y. P. Lu,[1,a] C. L. Luo,[28] M. X. Luo,[52] T. Luo,[42] X. L. Luo,[1,a] X. R. Lyu,[41] F. C. Ma,[27] H. L. Ma,[1] L. L. Ma,[33] M. M. Ma,[1] Q. M. Ma,[1] T. Ma,[1] X. N. Ma,[30] X. Y. Ma,[1,a] Y. M. Ma,[33] F. E. Maas,[14] M. Maggiora,[49a,49c] Q. A. Malik,[48] Y. J. Mao,[31] Z. P. Mao,[1] S. Marcello,[49a,49c] J. G. Messchendorp,[25] G. Mezzadri,[21b] J. Min,[1,a] T. J. Min,[1] R. E. Mitchell,[19] X. H. Mo,[1,a] Y. J. Mo,[6] C. Morales Morales,[14] N. Yu. Muchnoi,[9,e] H. Muramatsu,[43] P. Musiol,[4] Y. Nefedov,[23] F. Nerling,[10] I. B. Nikolaev,[9,e] Z. Ning,[1,a] S. Nisar,[8] S. L. Niu,[1,a] X. Y. Niu,[1] S. L. Olsen,[32] Q. Ouyang,[1,a] S. Pacetti,[20b] Y. Pan,[46,a] P. Patteri,[20a] M. Pelizaeus,[4] H. P. Peng,[46,a] K. Peters,[10,i] J. Pettersson,[50] J. L. Ping,[28] R. G. Ping,[1] R. Poling,[43] V. Prasad,[1] H. R. Qi,[2] M. Qi,[29] S. Qian,[1,a] C. F. Qiao,[41] L. Q. Qin,[33] N. Qin,[51] X. S. Qin,[1] Z. H. Qin,[1,a] J. F. Qiu,[1] K. H. Rashid,[48] C. F. Redmer,[22] M. Ripka,[22] G. Rong,[1] Ch. Rosner,[14] X. D. Ruan,[12] A. Sarantsev,[23,f] M. Savrié,[21b] C. Schnier,[4] K. Schoenning,[50] W. Shan,[31] M. Shao,[46,a] C. P. Shen,[2] P. X. Shen,[30] X. Y. Shen,[1] H. Y. Sheng,[1] W. M. Song,[1] X. Y. Song,[1] S. Sosio,[49a,49c] S. Spataro,[49a,49c] G. X. Sun,[1] J. F. Sun,[15] S. S. Sun,[1] X. H. Sun,[1] Y. J. Sun,[46,a] Y. Z. Sun,[1] Z. J. Sun,[1,a] Z. T. Sun,[19] C. J. Tang,[36] X. Tang,[1] I. Tapan,[40c] E. H. Thorndike,[44] M. Tiemens,[25] I. Uman,[40d] G. S. Varner,[42] B. Wang,[30] B. L. Wang,[41] D. Wang,[31] D. Y. Wang,[31] K. Wang,[1,a] L. L. Wang,[1] L. S. Wang,[1] M. Wang,[33] P. Wang,[1] P. L. Wang,[1] W. Wang,[1,a] W. P. Wang,[46,a] X. F. Wang,[39] Y. Wang,[37] Y. D. Wang,[14] Y. F. Wang,[1,a] Y. Q. Wang,[22] Z. Wang,[1,a] Z. G. Wang,[1,a] Z. H. Wang,[46,a] Z. Y. Wang,[1] Z. Y. Wang,[1] T. Weber,[22] D. H. Wei,[11] P. Weidenkaff,[22] S. P. Wen,[1] U. Wiedner,[4] M. Wolke,[50] L. H. Wu,[1] L. J. Wu,[1] Z. Wu,[1,a] L. Xia,[46,a] L. G. Xia,[39] Y. Xia,[18] D. Xiao,[1] H. Xiao,[47] Z. J. Xiao,[28] Y. G. Xie,[1,a] Y. H. Xie,[6] Q. L. Xiu,[1,a] G. F. Xu,[1] J. J. Xu,[1] L. Xu,[1] Q. J. Xu,[13] Q. N. Xu,[41] X. P. Xu,[37] L. Yan,[49a,49c] W. B. Yan,[46,a] W. C. Yan,[46,a] Y. H. Yan,[18] H. J. Yang,[34,j] H. X. Yang,[1] L. Yang,[51] Y. X. Yang,[11] M. Ye,[1,a] M. H. Ye,[7] J. H. Yin,[1] Z. Y. You,[38] B. X. Yu,[1,a] C. X. Yu,[30] J. S. Yu,[26] C. Z. Yuan,[1] Y. Yuan,[1] A. Yuncu,[40b,b] A. A. Zafar,[48] Y. Zeng,[18] Z. Zeng,[46,a] B. X. Zhang,[1] B. Y. Zhang,[1,a] C. C. Zhang,[1] D. H. Zhang,[1] H. H. Zhang,[38] H. Y. Zhang,[1,a] J. Zhang,[1] J. J. Zhang,[1] J. L. Zhang,[1] J. Q. Zhang,[1] J. W. Zhang,[1,a] J. Y. Zhang,[1] J. Z. Zhang,[1] K. Zhang,[1] L. Zhang,[1] S. Q. Zhang,[30] X. Y. Zhang,[33] Y. Zhang,[1] Y. Zhang,[1] Y. H. Zhang,[1,a] Y. N. Zhang,[41] Y. T. Zhang,[46,a] Yu Zhang,[41] Z. H. Zhang,[6] Z. P. Zhang,[46] Z. Y. Zhang,[51] G. Zhao,[1] J. W. Zhao,[1,a] J. Y. Zhao,[1] J. Z. Zhao,[1,a] Lei Zhao,[46,a] Ling Zhao,[1] M. G. Zhao,[30] Q. Zhao,[1] Q. W. Zhao,[1] S. J. Zhao,[53] T. C. Zhao,[1] Y. B. Zhao,[1,a] Z. G. Zhao,[46,a] A. Zhemchugov,[23,c] B. Zheng,[14,47] J. P. Zheng,[1,a] W. J. Zheng,[33] Y. H. Zheng,[41] B. Zhong,[28] L. Zhou,[1,a] X. Zhou,[51] X. K. Zhou,[46,a] X. R. Zhou,[46,a] X. Y. Zhou,[1] K. Zhu,[1] K. J. Zhu,[1,a] S. Zhu,[1] S. H. Zhu,[45] X. L. Zhu,[39] Y. C. Zhu,[46,a] Y. S. Zhu,[1] Z. A. Zhu,[1] J. Zhuang,[1,a] L. Zotti,[49a,49c] B. S. Zou,[1] and J. H. Zou[1]

(BESIII Collaboration)

[1]*Institute of High Energy Physics, Beijing 100049, People's Republic of China*
[2]*Beihang University, Beijing 100191, People's Republic of China*
[3]*Beijing Institute of Petrochemical Technology, Beijing 102617, People's Republic of China*
[4]*Bochum Ruhr-University, D-44780 Bochum, Germany*
[5]*Carnegie Mellon University, Pittsburgh, Pennsylvania 15213, USA*
[6]*Central China Normal University, Wuhan 430079, People's Republic of China*
[7]*China Center of Advanced Science and Technology, Beijing 100190, People's Republic of China*
[8]*COMSATS Institute of Information Technology, Lahore,*
Defence Road, Off Raiwind Road, Lahore 54000, Pakistan
[9]*G.I. Budker Institute of Nuclear Physics SB RAS (BINP), Novosibirsk 630090, Russia*
[10]*GSI Helmholtzcentre for Heavy Ion Research GmbH, D-64291 Darmstadt, Germany*
[11]*Guangxi Normal University, Guilin 541004, People's Republic of China*
[12]*Guangxi University, Nanning 530004, People's Republic of China*
[13]*Hangzhou Normal University, Hangzhou 310036, People's Republic of China*
[14]*Helmholtz Institute Mainz, Johann-Joachim-Becher-Weg 45, D-55099 Mainz, Germany*
[15]*Henan Normal University, Xinxiang 453007, People's Republic of China*
[16]*Henan University of Science and Technology, Luoyang 471003, People's Republic of China*
[17]*Huangshan College, Huangshan 245000, People's Republic of China*
[18]*Hunan University, Changsha 410082, People's Republic of China*
[19]*Indiana University, Bloomington, Indiana 47405, USA*
[20a]*INFN Laboratori Nazionali di Frascati, I-00044 Frascati, Italy*
[20b]*INFN and University of Perugia, I-06100 Perugia, Italy*
[21a]*INFN Sezione di Ferrara, I-44122 Ferrara, Italy*
[21b]*University of Ferrara, I-44122 Ferrara, Italy*
[22]*Johannes Gutenberg University of Mainz, Johann-Joachim-Becher-Weg 45, D-55099 Mainz, Germany*
[23]*Joint Institute for Nuclear Research, 141980 Dubna, Moscow region, Russia*
[24]*Justus-Liebig-Universitaet Giessen, II. Physikalisches Institut,*
Heinrich-Buff-Ring 16, D-35392 Giessen, Germany
[25]*KVI-CART, University of Groningen, NL-9747 AA Groningen, Netherlands*
[26]*Lanzhou University, Lanzhou 730000, People's Republic of China*
[27]*Liaoning University, Shenyang 110036, People's Republic of China*
[28]*Nanjing Normal University, Nanjing 210023, People's Republic of China*
[29]*Nanjing University, Nanjing 210093, People's Republic of China*
[30]*Nankai University, Tianjin 300071, People's Republic of China*
[31]*Peking University, Beijing 100871, People's Republic of China*
[32]*Seoul National University, Seoul 151-747, Korea*
[33]*Shandong University, Jinan 250100, People's Republic of China*
[34]*Shanghai Jiao Tong University, Shanghai 200240, People's Republic of China*
[35]*Shanxi University, Taiyuan 030006, People's Republic of China*
[36]*Sichuan University, Chengdu 610064, People's Republic of China*
[37]*Soochow University, Suzhou 215006, People's Republic of China*
[38]*Sun Yat-Sen University, Guangzhou 510275, People's Republic of China*
[39]*Tsinghua University, Beijing 100084, People's Republic of China*
[40a]*Ankara University, 06100 Tandogan, Ankara, Turkey*
[40b]*Istanbul Bilgi University, 34060 Eyup, Istanbul, Turkey*
[40c]*Uludag University, 16059 Bursa, Turkey*
[40d]*Near East University, Nicosia, North Cyprus, Mersin 10, Turkey*
[41]*University of Chinese Academy of Sciences, Beijing 100049, People's Republic of China*
[42]*University of Hawaii, Honolulu, Hawaii 96822, USA*
[43]*University of Minnesota, Minneapolis, Minnesota 55455, USA*
[44]*University of Rochester, Rochester, New York 14627, USA*
[45]*University of Science and Technology Liaoning, Anshan 114051, People's Republic of China*
[46]*University of Science and Technology of China, Hefei 230026, People's Republic of China*
[47]*University of South China, Hengyang 421001, People's Republic of China*
[48]*University of the Punjab, Lahore 54590, Pakistan*
[49a]*University of Turin, I-10125 Turin, Italy*
[49b]*University of Eastern Piedmont, I-15121 Alessandria, Italy*
[49c]*INFN, I-10125 Turin, Italy*
[50]*Uppsala University, Box 516, SE-75120 Uppsala, Sweden*
[51]*Wuhan University, Wuhan 430072, People's Republic of China*

^{52}Zhejiang University, Hangzhou 310027, People's Republic of China
^{53}Zhengzhou University, Zhengzhou 450001, People's Republic of China

The decays of $\chi_{c2} \to K^+ K^- \pi^0$, $K_S K^\pm \pi^\mp$, and $\pi^+ \pi^- \pi^0$ are studied with the $\psi(3686)$ data samples collected with the Beijing Spectrometer (BESIII). For the first time, the branching fractions of $\chi_{c2} \to K^* \bar{K}$, $\chi_{c2} \to a_2^\pm(1320)\pi^\mp / a_2^0(1320)\pi^0$, and $\chi_{c2} \to \rho(770)^\pm \pi^\mp$ are measured. Here, $K^* \bar{K}$ denotes both $K^{*\pm} K^\mp$ and its isospin-conjugated process $K^{*0} \bar{K}^0 +$ c.c., and K^* denotes the resonances $K^*(892)$, $K_2^*(1430)$, and $K_3^*(1780)$. The observations indicate a strong violation of the helicity selection rule in χ_{c2} decays into vector and pseudoscalar meson pairs. The measured branching fractions of $\chi_{c2} \to K^*(892)\bar{K}$ are more than ten times larger than the upper limit of $\chi_{c2} \to \rho(770)^\pm \pi^\mp$, which is so far the first direct observation of a significant U-spin symmetry breaking effect in charmonium decays.

The helicity selection rule (HSR) [1–3] is one of the most important consequences of perturbative quantum chromodynamics (pQCD) at leading twist accuracy. In the charmonium energy region, although there are observations that pQCD plays a dominant role, there are also many hints that nonperturbative mechanisms can become important [3–6]. Exclusive decays of the P-wave charmonium state $\chi_{c2} \to VP$, where V and P denote light vector and pseudoscalar mesons, respectively, are ideal for testing the HSR and pinning down the mechanisms that may violate the leading pQCD approximation.

Another reason the decays of $\chi_{c2} \to VP$ are of great interest is that this process is ideal for probing the long-range interactions arising from intermediate D-meson loop transitions. It was shown in Ref. [7] that the approximate G-parity or isospin conservation would further suppress the nonstrange intermediate D-meson loop transitions in the process of $\chi_{c2} \to \rho(770)^\pm \pi^\mp$. However, the U-spin symmetry breaking due to the relatively large mass difference between u/d and s quarks would lead to significant contributions from the intermediate charmed-strange D_s-meson loops in the decay of $\chi_{c2} \to K^*(892)\bar{K}$. Therefore, a precise measurement of these decays is of great value for our understanding of the physics in the interplay between the perturbative and nonperturbative QCD regimes, and the comparison between these two decays can provide a direct investigation into the role of the intermediate meson loops as a dominant mechanism for violating the HSR.

In this paper, we present a partial wave analysis (PWA) of the process $\chi_{c2} \to K\bar{K}\pi$ (denotes $K^+ K^- \pi^0$ and $K_S K^\pm \pi^\mp$) and a measurement of $\chi_{c2} \to \pi^+ \pi^- \pi^0$. We have two $\psi(3686)$ samples of $(107.0 \pm 0.8) \times 10^6$ (160 pb^{-1}) [8] and $(341.1 \pm 2.1) \times 10^6$ (510 pb^{-1}) [9] events collected in 2009 and 2012 by BESIII [10], respectively. Only the 2009 data sample is used in the analysis of $\chi_{c2} \to K\bar{K}\pi$, and the full data sample is used in $\chi_{c2} \to \pi^+ \pi^- \pi^0$ since it has a smaller branching fraction. An independent sample of about 44 pb^{-1} taken at $\sqrt{s} = 3.65$ GeV is utilized to investigate the potential background from the continuum process. A sample of Monte Carlo (MC) simulated events of generic $\psi(3686)$ decays (inclusive MC sample) is used to study backgrounds. The optimization of the event selection and the estimation of physics backgrounds are performed with Monte Carlo simulations of $\psi(3686)$ inclusive/exclusive decays.

The χ_{c2} candidates, produced in $\psi(3686)$ radiative decays, are reconstructed from the final states $K^+ K^- \pi^0$, $K_S K^\pm \pi^\mp$, and $\pi^+ \pi^- \pi^0$. Each charged track is required to have a polar angle θ in the main drift chamber (MDC) that satisfies $|\cos\theta| < 0.93$ and has the point of closest approach to the $e^+ e^-$ interaction point within 10 cm in the beam direction ($|V_z|$) and 1 cm in the plane perpendicular to the beam direction (V_r). The energy loss dE/dx in the MDC and the information from the time-of-flight system are combined to form particle identification (PID) confidence levels (C.L.) for the π, K, and p hypotheses, and each track is assigned with the hypothesis corresponding to the highest C.L. The K_S candidates are reconstructed from two oppositely charged tracks with loose vertex requirements ($|V_z| < 30$ cm and $V_r < 10$ cm) and without PID (assumed to be pions). Then the candidate with invariant mass closest to the K_S nominal mass and the decay length

provided by a secondary vertex fit algorithm greater than 0.25 cm is selected for further study in the decay $\psi(3686) \to \gamma K_S K^\pm \pi^\mp$. The candidate events are required to have two charged tracks with zero net charge, where the tracks from the K_S candidate are not taken into account. Two pions and one kaon are required for the decays $\psi(3686) \to \gamma \pi^+ \pi^- \pi^0$ and $\psi(3686) \to \gamma K_S K^\pm \pi^\mp$, respectively, and no PID requirement is applied for the decay $\psi(3686) \to \gamma K^+ K^- \pi^0$. The photon candidates are required to have energy larger than 25 (50) MeV in the Electromagnetic Calorimeter (EMC) barrel (end cap) region $|\cos\theta| < 0.8$ $(0.86 < |\cos\theta| < 0.93)$ and have an angle relative to the nearest charged tracks larger than 10°. To suppress electronic noise and energy deposits unrelated to the event, the EMC cluster time must be within 700 ns from the event start time. At least three photons and one photon are required for the decay $\psi(3686) \to \gamma \pi^+ \pi^- \pi^0 / K^+ K^- \pi^0$ and $\psi(3686) \to \gamma K_S K^\pm \pi^\mp$, respectively.

A fit with four kinematic constraints enforcing four-momentum conservation between the initial $\psi(3686)$ and the final state is performed for each process. If there are more photons than required in one event, all possible combinations of photons are considered, and only the one with the least χ_{4C}^2 of the kinematic fit is retained for further analysis. The χ_{4C}^2 is required to be less than 80 and 60 for the decays $\psi(3686) \to \gamma K^+ K^- \pi^0$ and $\psi(3686) \to \gamma K_S K^\pm \pi^\mp$, respectively. The π^0 candidate is reconstructed from the two selected photons of which the invariant mass is closest to the π^0 nominal mass and satisfies $|M_{\gamma\gamma} - M_{\pi^0}| < 10 \, \mathrm{MeV}/c^2$. For the decay mode $\psi(3686) \to \gamma \pi^+ \pi^- \pi^0$, a fit with five kinematic constraints is performed with an additional π^0 mass constraint, and $\chi_{5C}^2 < 60$ is required. To remove the backgrounds $\psi(3686) \to \pi^0 \pi^0 J/\psi$ $(J/\psi \to l^+ l^-$, $l = e, \mu)$, the invariant mass of $K^+ K^- / \pi^+ \pi^-$ is required to be less than $3.0 \, \mathrm{GeV}/c^2$ for the decay $\psi(3686) \to \gamma K^+ K^- \pi^0 / \gamma \pi^+ \pi^- \pi^0$. In the decay mode $\psi(3686) \to \gamma \pi^+ \pi^- \pi^0$, the π^0 recoil mass is required to be less than $3.0 \, \mathrm{GeV}/c^2$ to suppress the background $\psi(3686) \to \pi^0 J/\psi$, and $M_{\gamma\pi^0} \notin (0.7, 0.85) \, \mathrm{GeV}/c^2$ is required to veto the background $\psi(3686) \to \omega\pi^+\pi^-$ $(\omega \to \gamma\pi^0)$.

The $K\bar{K}\pi$ invariant masses for the decays $\psi(3686) \to \gamma K^+ K^- \pi^0$ and $\psi(3686) \to \gamma K_S K^\pm \pi^\mp$ are shown in Figs. 1(a) and 1(b), respectively. The $\chi_{c1,2}$ signals appear prominently with a small background. From the analysis of the $\psi(3686)$ inclusive MC sample and the continuum data at $\sqrt{s} = 3.65 \, \mathrm{GeV}$, the main backgrounds are from the decays $\psi(3686) \to \pi^0 \pi^0 J/\psi$ $(J/\psi \to \pi^+ \pi^- \pi^0 / \mu\mu)$ and $\psi(3686) \to K_1(1270)^\pm K^\mp$ $(K_1(1270)^\pm \to K^\pm \pi^0 \pi^0 / \rho(770)^\pm K_S)$. All of these backgrounds show a smooth distribution and do not produce a peak around the χ_{cJ} mass region. Unbinned maximum likelihood fits to the selected candidates are performed, in which the $\chi_{c1,2}$ signals are described with the MC simulated shapes convoluted with a Gaussian function accounting for the resolution difference between
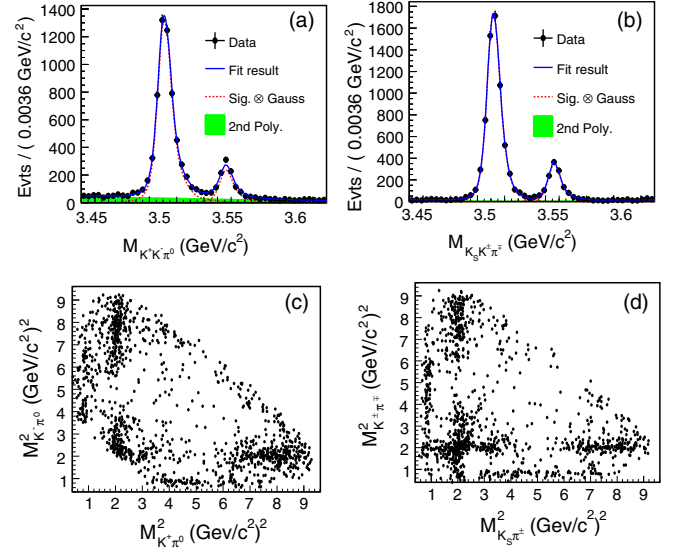

FIG. 1. Invariant mass distribution of (a) $K^+ K^- \pi^0$ and (b) $K_S K^\pm \pi^\mp$ for the decay $\psi(3686) \to \gamma K\bar{K}\pi$ and the corresponding Dalitz distributions (c) and (d) for the candidates within $|M_{KK\pi} - M_{\chi_{c2}}| < 15 \, \mathrm{MeV}/c^2$. The dots with error bars are for data, the blue solid curves are the overall fit results, the red dotted curves are the signals, and the green shaded areas are the background.

data and MC simulation, and the backgrounds are described with a second-order polynomial function. The total 1215 and 1176 candidate events for $\chi_{c2} \to K^+ K^- \pi^0$ and $\chi_{c2} \to K_S K^\pm \pi^\mp$ within the χ_{c2} signal region $|M_{K\bar{K}\pi} - M_{\chi_{c2}}| \leq 15 \, \mathrm{MeV}/c^2$ are used for PWA. Non-π^0 ($K^+ K^- \pi^0$ mode only) and non-χ_{c2} backgrounds are estimated with the events in the sideband regions, which are also used in the PWA as described in the following. The numbers of background events are estimated to be 240 and 80 for $\chi_{c2} \to K^+ K^- \pi^0$ and $\chi_{c2} \to K_S K^\pm \pi^\mp$, respectively.

In the PWA, the process $\chi_{c2} \to K\bar{K}\pi$ is assumed to proceed via the quasi-two-body decays, i.e. $\chi_{c2} \to a_2\pi$ and $K^*\bar{K}$ followed by $a_2 \to K\bar{K}$ and $K^* \to K\pi$. The amplitudes of the two-body decays are constructed with the helicity-covariant method [11]. For a particle decaying into two-body final states, i.e. $A(J, m) \to B(s, \lambda)C(\sigma, \nu)$, where spin and helicity are indicated in the parentheses, its helicity-covariant amplitude $F_{\lambda,\nu}$ [11] is (see supplemental material [12])

$$F_{\lambda,\nu} = \sum_{LS} A g_{LS} \langle L0S\delta | J\delta \rangle \langle s\lambda\sigma - \nu | S\delta \rangle r^L B_L(r), \quad (1)$$

where $A \equiv \sqrt{\frac{2L+1}{2J+1}}$, g_{LS} is the coupling constant for the partial wave with orbital angular momentum L and spin S (with z-projection δ), r is the relative momentum between the two daughter particles in the initial particle rest frame, and B_L is the barrier factor [13]. The conservation of parity

is applied in the equation. Recent measurements show that the contributions of higher-order magnetic and electric multipoles in the $\psi(3686)$ radiative transition to χ_{c2} are negligible, and the $E1$ transition is the dominant process [14]. Hence, the helicity amplitudes are constructed to satisfy the $E1$ transition relation [15] and parity conservation, namely, $F_{1,2} = \sqrt{2}F_{1,1} = \sqrt{6}F_{1,0}$ and $F_{0,0} = 0$. The corresponding g_{LS} are taken as complex values. The relative magnitudes and phases are determined by an unbinned maximum likelihood fit to data with the package MINUIT [16]. The background contribution to the likelihood value is estimated with the events in the sideband regions and is subtracted [17]. For the PWA method check, a set of input data is generated with the inclusion of all states in the baseline solution, and coupling constants are fixed to the PWA solution. After the detector simulation and selection criteria, the same PWA fit procedure is performed. Finally, the solution by the hypothesis tests can be found, even for the smaller component. For extra states which did not include in the input data, after our test, it still cannot be included into the baseline solution which just same as that in the input data. And then, the fit results are consistent with that of the input data within the statistical errors.

As shown in the Dalitz plots of Figs. 1(c) and 1(d), clear signals for $K^*(892)$ and $K_2^*(1430)$ are observed in the $K\pi$ system. The resonances $K^*(892)$ and $K_2^*(1430)$ in the $K\pi$ system as well as the $a_2(1320)$ in the $K\bar{K}$ system, which have a significance larger than 8σ in both decay modes, are included in the baseline solution. For insignificant excited K^* states, such as $K^*(1410)$, $K^*(1680)$, and $K_3^*(1780)$, their contributions are tested by the inclusion of their different combinations to the baseline solution. We find that the contribution from $K_3^*(1780)$ is quite stable (the difference is less than 10%), so it is included in the baseline solution. But it becomes unstable for the other two resonances (the difference is larger than 100%). Hence, $K^*(1410)$ and $K^*(1680)$ are excluded in the baseline solution, but they are considered as a source of systematic uncertainty. The coupling constants for the charge-conjugate modes are treated as the same.

Figures 2 and 3(a)–3(c) show the invariant mass distribution and the projection of the PWA for the decays $\chi_{c2} \to K^+K^-\pi^0$ and $\chi_{c2} \to K_S K^\pm \pi^\mp$, respectively. The signal yields for the individual processes with a given intermediate state and the corresponding statistical uncertainties are calculated according to the fit results. The resultant branching fractions for the decays $\chi_{c2} \to K^*\bar{K}$ and $\chi_{c2} \to a_2(1320)\pi$ are summarized in Table I. The branching fractions for the processes including charged K^* intermediate states are consistent between the two decay modes and are combined by considering the correlation of uncertainties between the two modes [18]. The K^* isospin-conjugated modes are consistent with each other within 2σ, as expected by isospin symmetry.

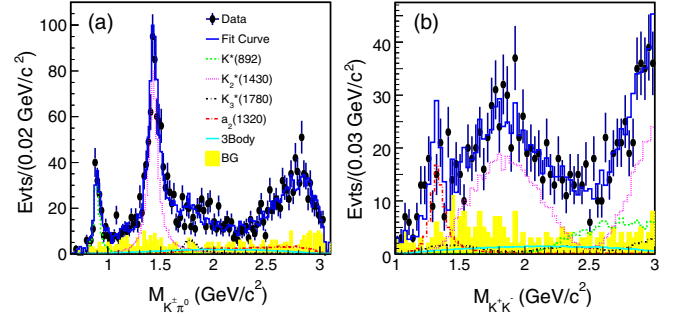

FIG. 2.   Projections of the fit results onto the invariant mass of (a) $K^\pm\pi^0$ and (b) K^+K^- in the decay $\chi_{c2} \to K^+K^-\pi^0$, where dots with error bars are for data, the blue solid histograms are the overall fit results, the yellow shaded histograms are for the background estimated using χ_{c2} sideband events, and the contributions from different components are indicated in the inset.

Note that the helicity amplitude ratios $|F_{2,0}|^2/|F_{1,0}|^2$, estimated with the fitted g_{LS} (see Table II), suggest the dominance of $F_{1,0}$ in the transition amplitudes. The amplitude $F_{1,0}$ contributes to the leading HSR violation effects and scales as $(\Lambda_{\rm QCD}/m_c)^6$ due to its asymptotic behavior [2,7], where $\Lambda_{\rm QCD} \sim 0.2$ GeV/c^2 and the charm quark mass $m_c \sim 1.5$ GeV/c^2. In comparison with the HSR conserved channel $\chi_{c2} \to VV$, which scales as $(\Lambda_{\rm QCD}/m_c)^4$, the ratio of $\chi_{c2} \to K_2^*(1430)\bar{K}$ to VV is expected to be suppressed by a factor of $(\Lambda_{\rm QCD}/m_c)^2 \sim 0.02$, However, the measured branching fraction of $\chi_{c2} \to K_2^*(1430)\bar{K}$ appears to be
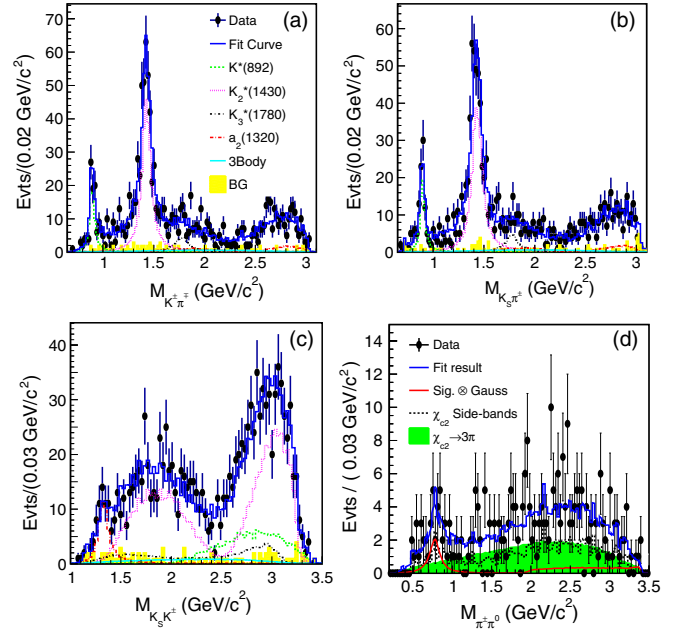

FIG. 3.   Projections of the fit results onto the invariant mass of (a) $K^\pm\pi^\mp$, (b) $K_S\pi^\pm$, and (c) $K_S K^\pm$ in the decay $\chi_{c2} \to K_S K^\pm \pi^\mp$ as well as (d) $\pi^\pm\pi^0$ in the decay $\chi_{c2} \to \pi^+\pi^-\pi^0$, where dots with error bars are for data, the blue solid histograms are the overall fit results, and the contributions from other components are indicated in the inset.

TABLE I. The measured branching fractions ($\times 10^{-4}$) for the decays $\chi_{c2} \to (K\pi)\bar{K}$ and $\chi_{c2} \to (K\bar{K})\pi$. The first uncertainties are statistical, and the second are systematic (Here, K^*, K_2^*, K_3^*, and a_2 refer to $K^*(892)$, $K_2^*(1430)$, $K_3^*(1780)$, and $a_2(1320)$, respectively)[a].

Mode	$K^+K^-\pi^0$	$K_S K^\pm \pi^\mp$	Combined
$K^{*\pm}K^\mp$	$1.8 \pm 0.2 \pm 0.2$	$1.4 \pm 0.2 \pm 0.2$	$1.5 \pm 0.1 \pm 0.2$
$K^{*0}\bar{K}^0$	$\cdots$	$1.3 \pm 0.2 \pm 0.2$	$\cdots$
$K_2^{*\pm}K^\mp$	$18.2 \pm 0.8 \pm 1.6$	$13.6 \pm 0.8 \pm 1.4$	$15.5 \pm 0.6 \pm 1.2$
$K_2^{*0}\bar{K}^0$	$\cdots$	$13.0 \pm 1.0 \pm 1.5$	$\cdots$
$K_3^{*\pm}K^\mp$	$5.3 \pm 0.5 \pm 0.9$	$5.9 \pm 1.1 \pm 1.5$	$5.4 \pm 0.5 \pm 0.7$
$K_3^{*0}\bar{K}^0$	$\cdots$	$5.9 \pm 1.6 \pm 1.5$	$\cdots$
$a_2^0\pi^0$	$13.5 \pm 1.6 \pm 3.2$	$\cdots$	$\cdots$
$a_2^\pm\pi^\mp$	$\cdots$	$18.4 \pm 3.3 \pm 5.5$	$\cdots$

[a]The extraction of the signal yields and the corresponding statistical uncertainties from the fit parameters is further explained in the supplement material [12].

the same order of magnitude as that for $\chi_{c2} \to VV$ [19], which indicates a significant violation of the HSR in $\chi_{c2} \to K_2^*(1430)\bar{K}$.

In the analysis of the decay $\psi(3686) \to \gamma\pi^+\pi^-\pi^0$, the χ_{c2} signal is extracted by the requirement $|M_{\pi^+\pi^-\pi^0} - M_{\chi_{c2}}| \leq 15$ MeV/c^2. The potential background from direct e^+e^- annihilation is found to be negligible by studying the continuum data taken at $\sqrt{s} = 3.65$ GeV. The backgrounds from $\psi(3686)$ decay are investigated with the $\psi(3686)$ inclusive MC sample; the only surviving χ_{c2} events are those that directly decay to $\pi^+\pi^-\pi^0$ without any intermediate state. There are also non-χ_{c2} backgrounds, which can be estimated by the events in the χ_{c2} sideband regions. Figure 3(d) shows the invariant mass of $\pi^\pm\pi^0$ for the selected candidates, together with the binned likelihood fit results. Here, the fit components include the $\rho(770)^\pm$ signal, the direct decay $\chi_{c2} \to \pi^+\pi^-\pi^0$, and the non-$\chi_{c2}$ background. The $\rho(770)^\pm$ signal and the direct χ_{c2} three-body decay are modeled with the MC simulated shapes convoluted with a Gaussian function with free parameters. The resonant parameters of the $\rho(770)^\pm$ are set to the values in the particle data group (PDG) [20]. The fitted signal yields are 14.7 ± 8.9 and 63.6 ± 13.0, and the corresponding resultant branching fractions are $(0.64 \pm 0.39 \pm 0.07) \times 10^{-5}$ and $(2.1 \pm 0.4 \pm 0.2) \times 10^{-5}$ for $\chi_{c2} \to \rho(770)^\pm\pi^\mp$ and the direct decay $\chi_{c2} \to \pi^+\pi^-\pi^0$, respectively, where the first uncertainties are statistical and the

TABLE II. The measured ratios of helicity amplitude squared $|F_{2,0}|^2/|F_{1,0}|^2$, where the uncertainties are statistical only.

	$K^+K^-\pi^0$	$K_S K^\pm \pi^\mp$	
	Charged K^*	Charged K^*	Neutral K^*
$K_2^*(1430)$	0.046 ± 0.001	0.042 ± 0.019	0.031 ± 0.018

second are systematic. Since the statistical significance for the $\chi_{c2} \to \rho(770)^\pm\pi^\mp$ is only 2.8σ, the upper limit at the 90% C.L. for the branching fraction is set to 1.1×10^{-5} by the method of the Feldman-Cousins approach with the systematic uncertainties consideration [21].

The uncertainties from the branching fractions of $\psi(3686) \to \gamma\chi_{c2}$, $K_S \to \pi^+\pi^-$, $\pi^0 \to \gamma\gamma$, $a_2(1320) \to K\bar{K}$, and $K^* \to K\pi$ are quoted from the PDG [20]. The uncertainty on the number of $\psi(3686)$ events is about 0.8% [8,9]. The uncertainties associated with the tracking and PID are 1% for every charged track [22]. The uncertainty related with EMC shower reconstruction efficiency is 1% per shower [22]. The uncertainties associated with the kinematic fit are estimated to be 0.5% and 0.6% for the 4C and 5C fits, respectively, by using a method to correct the charged-track helix parameters [23]. The uncertainty associated with the K_S reconstruction is estimated to be 2.5% [23]. The uncertainties related with the π^0 selection, the requirements on the π^0 recoil mass, and the ω background veto [in the $\chi_{c2} \to \rho(770)^\pm\pi^\mp$ mode only] are negligible.

In the decay $\chi_{c2} \to \rho(770)^\pm\pi^\mp$, the uncertainties due to the bin size and the fit range in the fit are estimated by repeating the fit with alternative bin sizes and fit ranges. The uncertainty due to the shape of $\chi_{c2} \to \pi^+\pi^-\pi^0$ is estimated by replacing the MC simulated line shape with a third polynomial function. The uncertainty due to the shape of the background is estimated by changing the χ_{c2} sideband regions.

In the decay $\chi_{c2} \to K\bar{K}\pi$, the uncertainties due to the contribution from $K^*(1410)$ and $K^*(1680)$ are estimated by including these states in the fit. The uncertainties associated with the backgrounds are determined by changing the χ_{c2} and π^0 sideband regions. The spin density matrix corresponding to the $E1$ transition [15] is used in the nominal fit. To estimate the uncertainty, contributions from the quadrupole ($M2$) and other high-order multipoles to the matrix [14] are included in the fit, and the changes in the final results are treated as a systematic uncertainty. The uncertainties associated with the resonance parameters of intermediate states are estimated by varying their values by 1σ of their uncertainties quoted in the PDG [20]. The uncertainty due to the barrier radius [13] when calculating $B_L(r)$ in Eq. (1) is estimated by alternative fits with $r = 0.25$ or 0.75 fm, respectively, where $r = 0.6$ fm is the nominal value. The uncertainty associated with the direct three-body decay $\chi_{c2} \to K\bar{K}\pi$ is estimated by alternative fits with other spin-parity hypotheses, e.g. a 0^- or 3^- nonresonant component in the $K\bar{K}$ or $K\pi$ systems. The largest changes in the signal yields are taken as systematic uncertainties. Assuming all the systematic errors are independent, the overall systematic is obtained by taking the quadrature sum of the individual values.

In summary, the HSR suppressed processes of $\chi_{c2} \to K_2^*(1430)\bar{K}$, $\chi_{c2} \to K^*(892)\bar{K}$, and $\chi_{c2} \to \rho(770)^\pm\pi^\mp$ are

studied with the $\psi(3686)$ data collected by BESIII for the first time. The branching fractions of $\chi_{c2} \to K^*(892)^{\pm}K^{\mp}$, $\chi_{c2} \to K^*(892)^0\bar{K}^0 +$c.c., $\chi_{c2} \to K_2^*(1430)^{\pm}K^{\mp}$, and $\chi_{c2} \to K_2^*(1430)^0\bar{K}^0 +$c.c. are measured to be $(1.5 \pm 0.1 \pm 0.2) \times 10^{-4}$, $(1.3 \pm 0.2 \pm 0.2) \times 10^{-4}$, $(15.5 \pm 0.6 \pm 1.2) \times 10^{-4}$, and $(13.0 \pm 1.0 \pm 1.5) \times 10^{-4}$, respectively. As estimated above, the branching fraction for the amplitude $F_{1,0}$ dominant process is excepted to be suppressed by a factor of 0.02 to those of the HSR conserving decay $\chi_{c2} \to VV$. However, by comparing our measurement with that of $\chi_{c2} \to VV$ in Refs. [19,20], they are rather sizeable for our measurement. The large branching fractions of $\chi_{c2} \to K_2^*(1430)\bar{K}$ and $\chi_{c2} \to K^*(892)\bar{K}$ are a direct indication of the significant HSR violation effects. These branching fractions of $\chi_{c2} \to K^*(892)\bar{K}$ are at least 1 order of magnitude larger than the upper limit of the branching fraction of $\chi_{c2} \to \rho(770)^{\pm}\pi^{\mp}$ (1.1×10^{-5}). It is worth noting that this phenomenon is anticipated by the HSR violation mechanism proposed in Ref. [7]. Namely, the HSR violation in $\chi_{c2} \to K^*(892)\bar{K}$ occurs via the intermediate meson loops due to the large U-spin symmetry breaking, while that in $\chi_{c2} \to \rho(770)^{\pm}\pi^{\mp}$ is due to isospin symmetry breaking. Due to the large mass difference between s and u/d quarks, the U-spin symmetry is broken more severely in comparison with isospin symmetry. This results in the larger decay branching for $\chi_{c2} \to K^*(892)\bar{K}$ than that for $\chi_{c2} \to \rho(770)^{\pm}\pi^{\mp}$. The results are crucial for further quantifying the HSR violation mechanisms [7] and also provide deeper insights into the underlying strong interaction dynamics in the charmonium energy region.

ACKNOWLEDGMENTS

[1] S. J. Brodsky and G. P. Lepage, Phys. Rev. D **24**, 2848 (1981).

[2] V. L. Chernyak and A. R. Zhitnitsky, Nucl. Phys. **B201**, 492 (1982); **B214**, 547(E) (1983).

[3] V. L. Chernyak and A. R. Zhitnitsky, Phys. Rep. **112**, 173 (1984).

[4] N. Brambilla et al. (Quarkonium Working Group), arXiv:hep-ph/0412158.

[5] M. B. Voloshin, Prog. Part. Nucl. Phys. **61**, 455 (2008).

[6] D. M. Asner et al. Int. J. Mod. Phys. A **24**, 1 (2009).

[7] X. H. Liu and Q. Zhao, Phys. Rev. D **81**, 014017 (2010).

[8] M. Ablikim et al. (BESIII Collaboration), Chin. Phys. C **37**, 063001 (2013).

[9] M. Ablikim et al. (BESIII Collaboration), arXiv:1709.03653.

[10] M. Ablikim et al. (BESIII Collaboration), Nucl. Instrum. Methods Phys. Res., Sect. A **614**, 345 (2010).

[11] S. U. Chung, Phys. Rev. D **57**, 431 (1998); **48**, 1225 (1993).

[12] See Supplemental Material at http://link.aps.org/supplemental/10.1103/PhysRevD.96.111102 for detailed description of the PWA process.

[13] B. S. Zou and D. V. Bugg, Eur. Phys. J. A **16**, 537 (2003).

[14] M. Ablikim et al. (BESIII Collaboration), Phys. Rev. D **84**, 092006 (2011).

[15] G. Karl, J. Meshkov, and J. L. Rosner, Phys. Rev. D **13**, 1203 (1976).

[16] F. James, CERN Program Library Long Writeup D 506 (1998).

[17] M. Ablikim et al. (BESIII Collaboration), Phys. Rev. D **86**, 072011 (2012).

[18] G. D'Agostini, Nucl. Instrum. Methods Phys. Res., Sect. A **346**, 306 (1994).

[19] M. Ablikim *et al.* (BESIII Collaboration), Phys. Rev. Lett. **107**, 092001 (2011).

[20] K. A. Olive *et al.* (Particle Data Group), Chin. Phys. C **38**, 090001 (2014).

[21] J. Conrad, O. Botner, A. Hallgren, and C. Pérez de los Heros Phys. Rev. D **67**, 012002 (2003).

[22] M. Ablikim *et al.* (BESIII Collaboration), Phys. Rev. D **83**, 112005 (2011).

[23] M. Ablikim *et al.* (BESIII Collaboration), Phys. Rev. D **87**, 012002 (2013).